PLOS COMPLEX SYSTEMS

RESEARCH ARTICLE

Just in time vs. all in sync: An analysis of two types of synchronization in a minimal model of machine activity in industrial production

Sanghita Bose[1]*, **Annick Lesne**[2,3], **Julia Arlinghaus**[4], **Marc-Thorsten Hütt**[1]

1 School of Science, Constructor University Bremen, Germany, **2** Sorbonne Université, CNRS, Laboratoire de Physique Théorique de la Matière Condensée, LPTMC, F-75252, Paris, France, **3** Institut de Génétique Moléculaire de Montpellier, University of Montpellier, CNRS, F-34293, Montpellier, France, **4** Otto-von-Guericke University Magdeburg, Universitätsplatz 2, 31904, Magdeburg, Germany

* sbose@constructor.university

Citation: Bose S, Lesne A, Arlinghaus J, Hütt M-T (2025) Just in time vs. all in sync: An analysis of two types of synchronization in a minimal model of machine activity in industrial production. PLOS Complex Syst 2(2): e0000033. https://doi.org/10.1371/journal.pcsy.0000033

Editor: Jaehee Kim, Cornell University, UNITED STATES OF AMERICA

Received: April 3, 2024

Accepted: December 9, 2024

Published: February 18, 2025

Data Availability Statement: All relevant data are within the manuscript and its Supporting information files.

Funding: MH and JA acknowledge support by Deutsche Forschungsgemeinschaft (DFG) (grant numbers BE 6322/4-1 and HU 937/27-1). MH thanks LPTMC (Paris, Sorbonne Université and CNRS UMR 7600) for hospitality and the Physics Institute of CNRS (French National Center for Scientific Research) for funding his stays, during which part of this work was performed. The

Abstract

The notion of synchronization in logistics is distinct from that encountered in the natural sciences and, in particular, in physics where synchronization rather means that the different parts of the system operate in unison. In logistics, synchronization is often associated with a 'just in time' paradigm in supply and production systems. A perfect logistics synchronization therefore is that the activity in a process triggers activity in a neighboring process without delay or queuing. Globally, this type of synchronization can be envisioned as a wave of activity running through the logistics chain. Our goal is a deeper theoretical understanding of these two types of synchronization, i.e. physics synchronization and logistics synchronization, as well as their interplay in the context of production systems where both types may coexist. We employ a minimal model of propagating excitations (representing machine activity) in a graph (representing a production network where each node is a machine). We evidence a strong change in the relationship between the two types of synchronization as a function of two parameters: the machine setup time and the random machine activation representing scheduling conflicts. Comparison of numerical results with pair-approximation mean-field predictions gives mechanistic insights into the synchronization behavior. Using robustness against network connectivity failures as a performance indicator, we find that, depending on the dynamical regime and network architecture, both logistics and physics synchronization can serve as easy-to-measure indicators of systemic performance.

Author summary

Synchronization in production systems is seen as having either a positive effect, as it leads to streamlined workflows, minimized variability, and optimized resource utilization, or a negative effect, as it may render production systems more susceptible to disruption. We address this debate by analyzing synchronization in a network of machines using a minimal model of machine activity. We distinguish two types of synchronization, one relying on sequential activation of machines and implementing a 'just in time' paradigm found in

funders had no role in study design, data collection and analysis, decision to publish, or preparation of the manuscript.

Competing interests: The authors have declared that no competing interests exist.

logistics, the other based on parallel activation of machines and closer to the notion of synchronization found in physics. We study the coexistence of these two types of synchronization as a function of two parameters: the machine setup time and the conflicts with other jobs running on the same machines, resulting in random activation. Our results show both an antagonistic relationship between the two forms of synchronization at low conflict rate and long setup times, and a correlated relationship at high conflict rate or short setup times. Using the average activity change under edge removal as a key performance indicator (KPI), we find a similarly rich dependence of this indicator as a function of the system parameters.

Introduction

In natural sciences, the term 'synchronization' is understood in relation to the parts of a system and their respective rhythms. It is one of the best investigated phenomena in the theory of dynamical systems with prominent modern contributions by [1–3] and many others [see also [4, 5]]. One of the most established definitions is given by [5] where it is stated that synchronization is "the adjustment of rhythms due to interaction". [6] defined synchronization similarly "as the capacity of objects of different nature to form a common operation regime due to interaction or forcing". These definitions are used to describe synchronization phenomena in various disciplines with the common feature that different types of objects or systems exhibit a harmonious ensemble behavior triggered by some interaction. For instance, synchronization of a system of coupled nonlinear oscillators is defined as all oscillators operating in unison. It emerges when the coupling strength is higher than a critical value. Using the vocabulary from the theory of self-organization (see, e.g., [7]) and from synergetics (see, e.g., [8]), the amount of synchronization can be seen as the order parameter of the system. Under the change of a control parameter (the coupling strength), the order parameter changes discontinuously. The term "emergence" precisely implies this spontaneous onset of a particular pattern (in this case, synchronization), when a control parameter is changed. The recent review article on one of the most important minimal models of synchronization, the Kuramoto model, shows the wide range of applications of synchronization [9]. For example, over the last few years, this notion of synchronization has become a new key approach for understanding extended failures in power grids and for designing robust power grid systems [10, 11].

The concept of synchronization can also be envisioned in the context of logistics, however major differences appear. Production companies constantly seek for new approaches to successfully deal with the complex and dynamic framework conditions arising from global markets and competition. The dissemination of powerful information and communication technology makes the resulting cost and quality differences more transparent to the (end-)customers. This leads the attention of production managers towards acknowledged logistics performance parameters, namely lead time, inventory levels, due date reliability, capacity utilization as well as more innovative measures, such as flexibility and robustness [12–19]. Many production companies have introduced concepts such as Lean Management and Just-in-Time to reach the necessary operational excellence and high flexibility reflected by low inventory levels, short lead times and high due-date reliability [20]. Within the mindset of the *lean management* philosophy, how the optimal timing of material flows across logistics systems improves logistics performance is perceived to be one "key to competitiveness and survival" [see for instance [21]]. A wide range of research activities on coordinated material flows emerged in the fields of production logistics and supply chain management [14, 15]. Several

authors have shown that a proper coordination can improve the performance and efficiency of logistics and manufacturing systems [see for instance [21–23]]. In these research streams, synchronization is thus defined as the coordination of material flows between manufacturing or logistics systems. For instance, in job-shop environments, synchronization of material flows is expected to reduce work-in-process inventories and lead times [14, 15] and thus to increase manufacturers' due-date performance [12, 13].

Moreover, two contrasting approaches ('push' and 'pull') are used to manage the flow of materials and products across the production process. In a 'push' system, production is based on demand projections or predetermined schedules and products are produced and supplied in anticipation of demand. This forward wave of activity thus involves proactive production in anticipation of future demand. A 'pull' system follows the 'just-in-time' model, where goods are produced only when there is a demand or an order, and materials and supplies are ordered only when needed. This backward wave of activity involves reacting to real time demand signals triggering upstream processes.

One example of synchronization in logistics systems is the production synchronous supply, known as *just-in-time* delivery, and is an integral part of the lean management philosophy. Pre-assembled modules and systems, such as doors, seats or engines, are produced and delivered only with a few hours' notice from the supplier to the original equipment manufacturers [24, 25]. Another example of synchronization in manufacturing systems is the paced assembly line. This specific delivery concept is the counterpart of an example of synchronization in manufacturing systems- the "takted" (rhythm) assembly line. Both concepts first emerged in automotive industry and are increasingly implemented in aviation, machinery and electronics industry and also, in an adapted form, in the distribution networks of fast-moving-consumer-goods industry. In a takted assembly line, all workstations have the same amount of time to execute a specific set of tasks allocated to them [26]; this *takt* or *cycle time* acts as the pacemaker and allows the products to move "in sync". In this respect, synchronization in logistics and manufacturing can be associated with flow orientation, as already pointed out by [27] in his landmark book *Toyota Production System*, referring to just-in-time manufacturing as "this flow".

In logistics and manufacturing, the logistics synchronization or sequential coordination is perceived as a system characteristic actively created and desired. It is perceived to have mainly positive effects on the system performance. Although many authors have also shown that there are drawbacks arising from close coupling of takted assembly lines [28, 29] and global production systems [see for instance [30–32]], synchronization is mainly perceived as a positive system feature, as indicated by the wide application of lean manufacturing principles [see for instance [33]].

In [34], it was first observed that physics synchronization strongly affects these common features of logistics systems: For the case of train schedules, the authors showed that high synchronization often goes along with high efficiency, but low robustness. In the broader context of logistics systems, physics synchronization has been applied to traffic light control [35, 36] and to diverse collective patterns emerging in the self-organization of traffic [37–39]. In [40], traffic control and the control of production systems are compared from the perspective of physics synchronization. These findings on negative effects of synchronization question the well-accepted assumption that logistics synchronization leads to higher efficiency in manufacturing systems.

An important development over the last 15 years in the theory of synchronization has been the wide range of studies about synchronization in complex networks. Tight relationships have been discovered between the synchronizability of networks and the global architectural features of the network: the network's *topology* [41]. For instance, quasi-stable states at

intermediate synchronization levels have been discovered and topologically understood in hierarchical graphs [42]. For interdependent networks, a novel theoretical framework has been formulated over the last few years in the context of statistical physics, which has a high potential of application to manufacturing systems. A striking work [43] has shown how interdependencies of networks drastically enhance their vulnerability to random failures [see also [44–46]].

The two types of synchronization, namely logistics and physics synchronization, are easy to measure in standard production (machine activity) data. There is evidence relating logistics synchronization with due-date reliability [47] and physics synchronization with vulnerability [34]. Also the impact of production parameters on both types of synchronization has been studied in detail [48]. However, the basic question, whether these two quantities are typically mutually exclusive or can jointly occur in a system, has not been addressed. Here we study the generic relationship between the two types of synchronization in a simple dynamical model, propagating excitations in a graph, mimicking machine activity in a production network. In the following, we thus study the general relationship between the two types of synchronization keeping in mind that there is no 'conservation law' here regarding the amount of activity in the network, so that physics and logistics synchronization are not interlinked in a zero-sum game. In particular, we investigate numerically which type of synchronization dominates as a function of the two main parameters of the model: machine setup time, described via the recovery probability p after an active phase, and conflicts with other production tasks or alternative products manufactured on the same production line, represented by the rate of spontaneous activation, f.

Using pair approximation, we derive mean-field expression for logistics and physics synchronization measures, and study how these mean-field proxies are affected by parameter changes. Comparison of these mean-field proxies with simulation results give mechanistic insights into the synchronization behavior.

Furthermore, we study the impact of these distinct types of synchronization on our proxies of key performance indicators. Lastly we outline how our findings can be subsequently validated using empirical data.

Methods

SER model

Minimal models have been used for long in theoretical physics and the field of complex systems to capture the determinants of a real world system as seen in works by [49] and [50]. Even though a detailed, parameter-rich and high-dimensional model is essential for realistic predictions and accurate planning of manufacturing processes, minimal models incorporating only the dominant mechanisms and a small number of parameters are needed for understanding the generic properties common to manufacturing systems. The minimal model of activity in a logistic network used here is a 3-state stochastic cellular automaton with two parameters: the recovery probability p (representing machine latency or machine setup time) and the rate of spontaneous machine activation f, representing (an often small percentage of) random orders being processed in the same production network or baseline activity. The machine setup time is the duration needed to prepare a machine for its next production run after it has completed the last part of the previous run. The stochastic recovery process with probability p yields a geometric distribution of setup times with average $1/p$ and standard deviation $\sqrt{(1-p)}/p$. This model has been originally studied as a model of self-organized criticality in [51], and later been applied to address abstract questions of excitable dynamics on graphs in [52]. Each node (i.e., each machine) in the network can be in a susceptible (or idle) state S, or

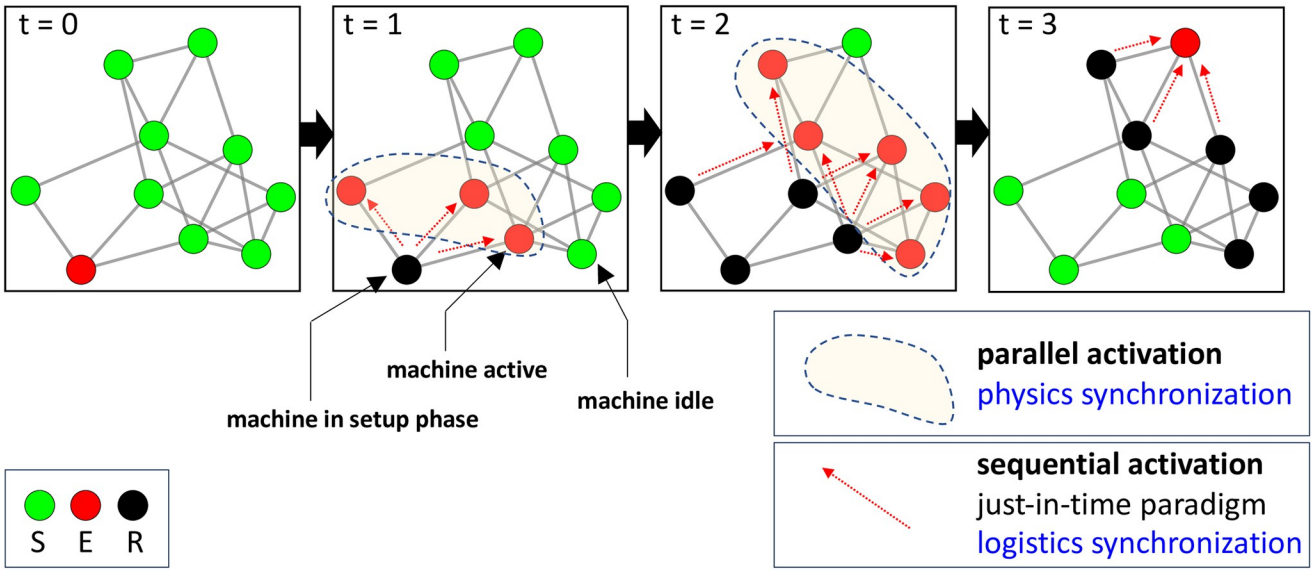

Fig 1. Schematic representation of physics (parallel) and logistics (sequential) synchronization arising in a minimal model of excitable dynamics on graphs.

https://doi.org/10.1371/journal.pcsy.0000033.g001

an excited (or active) state *E*, or a refractory (or resetting) state *R*. The update rules are the following:

(1) A node in the susceptible state *S* changes into an excited node *E* if one or more of its neighbors is excited. Alternatively, a node can go from *S* to *E* in a stochastic way with a given rate of spontaneous activation, *f*. (2) A node in the excited state *E* changes into a node in the refractory state *R*. (3) A node in the refractory state *R* changes into a node in the susceptible state *S* in a stochastic way with a given recovery probability *p*.

The SER model used here is conceptually similar to the well-known class of toy models used in the study of epidemic propagation (see [53]), like SIS, SIR and SIRS. However, in the SER model the transmission of activity is deterministically controlled by neighboring nodes with the exception of random spontaneous excitations acting as noise, whereas in the SIR models excitation transmission is stochastic and characterized by a transmission probability. Another difference is that machine recovery is a probabilistic step in the SER model, and not in the the SIR models.

Fig 1 displays a sketch of the two different types of synchronization that can be observed in this minimal model, and interpreted as the notions of logistics and physics synchronization described in introduction. Each network in the diagram represents a production network at different time points, in which each node represents a work station. The nodes are updated synchronously according to the above rules. Physics (parallel) synchronization originates from simultaneous activation of machines in the network whereas logistics (sequential) synchronization arises from the sequential activity and trigger of nodes by the previous node, representing an upstream machine. For the quantitative analysis, we single out excited states, and map the local state of node *i* at time *t* to {1, 0} where 1 denotes excitation (state *E*) and 0 denotes no excitation (states *S* or *R*), in order to obtain a new time series composed of 0 and 1.

Measure for the two types of synchronization

Logistics and physics synchronization have been previously quantified in [47], as follows.

Measures for logistics synchronization. Logistics synchronization is defined as the coordinated activity of machines that are linked by material flows.

A proper measure has to describe how much activity in a machine has been triggered by the upstream machine. The quantification of logistics synchronization from [47] can be adapted to numerical simulations of the above-described SER model in the following way. The standard cross-correlation between the activity of machine i and the activity of machine j is computed as:

$$c_{i,j}(\tau) = \frac{1}{N-\tau}\sum_{t=1}^{N-\tau}\left(\frac{i_t - \bar{i}}{\sigma_i}\right)\left(\frac{j_{t+\tau} - \bar{j}}{\sigma_j}\right), \tag{1}$$

where $\bar{i}, \bar{j}$ and σ_i, σ_j are the mean and standard deviation of the time series at nodes i and j respectively, while the parameter τ is the time delay and N is the length of the time series.

The maximal value over the time delay τ of these cross-correlation coefficients is computed for all pairs of machines in the network, including the unconnected pairs:

$$c^*_{i,j} = \max_{\tau>0} \ |c_{i,j}(\tau)|. \tag{2}$$

For a system to exhibit high logistics synchronization, the machines that are connected to each other (the edges representing a material flow $i \longrightarrow j$ between the machines i, j) should be more synchronized than the unconnected machines. The logistics synchronization index is thus formulated as the ratio between the cross-correlation averaged over the L connected pairs of machines and the cross-correlation averaged over the M possible pairs a, b:

$$\sigma_L = \frac{\frac{1}{L}\sum_{i\to j} c^*_{i,j}}{\frac{1}{M}\sum_{a,b} c^*_{a,b}}, \tag{3}$$

where $M = \frac{z(z-1)}{2}$, z is the total number of machines in the network. For the SER model used here, the main contribution to the cross-correlation c^*_{ij}, comes from time delays $\tau = 1$, corresponding to repeated observations of sequential activation of the nodes i and j. The logistics synchronization index σ_L quantifies the excess in sequential activation of connected nodes, compared to random pairs of nodes in the network. This normalization avoids spurious sensitivity when the number of non-connected machines is small. It corresponds to what in neuroscience [54] and other fields [55] is referred to as the agreement between structural and functional connectivity (or SC/FC correlation). The definition of logistics synchronization has been designed ([47]) for general production data. Values can be interpreted as measuring the excess in correlation for connected pairs of machines, compared to all machine pairs. A value of $1 + q$, $q > 0$ thus indicates that connected machines show sequential activation $100q$ percent more often than random pairs of machines.

Measure for physics synchronization. In the present context, physics synchronization is defined as the parallel activity existing in the production network when machines are activated in unison. We adapt the quantification of physics synchronization described in [47] to the simulations in the following way: The phases are obtained by mapping the differences between order arrival times to a phase interval of 2π. Namely, the phase of machine n at a given time point t_l is calculated as

$$\phi^n_l = 2\pi\frac{t_l - t^{(n)}_j}{t^{(n)}_{j+1} - t^{(n)}_j}, \tag{4}$$

where $t^{(n)}_j$ is the last operation start time before time t_l and $t^{(n)}_{j+1}$ is the first operation start time

after time t_l. The physics synchronization index is then calculated as:

$$\sigma_P = \left| \frac{1}{z} \sum_{n=1}^{n=z} e^{i\phi_l^n} \right|. \tag{5}$$

Mean-field analysis

We have developed two mean-field approaches (standard and pair-approximation) to describe analytically how state densities depend on the parameters of excitable dynamics.

These approaches have been previously described in [56], and here adapted for the analysis of synchronization. Comparing mean-field predictions with numerical simulations of SER dynamics on graphs provides a mechanistic insight, of which features and patterns of the dynamics can be explained without taking into account correlations between the nodes, or only pairwise correlations. The nodes of the (undirected and unweighted) graph in the present dynamical model can be in states *S*, *E* and *R*. A first point in the mean-field approach is to describe the system in terms of the probability of each local state, in a space-implicit description. These probabilities are identified with 1-node densities:

$$c_\alpha(i,t) = \text{Prob}[s_i(t) = \alpha], \tag{6}$$

where $s_i(t)$ denotes the state of node *i* at discrete time t with $\alpha = S$, *E* or *R*. Standard (first-order) mean-field approach assumes that node states are independent (i.e. correlations between nodes are completely ignored) and that c_α does not depend on the node *i*. We denote:

$$\theta(t) = [1 - c_E(t)]. \tag{7}$$

The first mean-field approximation identifies the probability that a neighbor is not excited with the average and node-independent quantity $1 - c_E(t)$. According to the second approximation (homogenization), the degree of each node is replaced with the average degree of the network denoted by $\langle k \rangle$. The closed set of evolution equations for the 1-node densities are [56]:

$$\begin{aligned} c_E(t+1) &= c_S(t)[f + (1-f)[1 - \theta(t)^{<k>}]] \\ c_R(t+1) &= c_E(t) + (1-p)c_R(t) \\ c_S(t+1) &= pc_R(t) + (1-f)\theta(t)^{<k>} c_S(t). \end{aligned} \tag{8}$$

S1 Fig illustrates these equations in the form of a transition graph among the SER states. The pair-approximation (second-order) mean-field approach still assumes spatial homogeneity, but now pair correlations are considered. We introduce pair densities, identified with joint probabilities according to:

$$c_{\alpha,\beta}(i,j,t) = \text{Prob}[s_i(t) = \alpha, s_j = \beta]. \tag{9}$$

A first mean-field approximation assumes that $c_{\alpha,\beta}(i,j,t) = c_{\alpha,\beta}^{nn}$ for any pair of nearest neighbors on the graph (nodes connected by a direct link). The correlations between the target node and its other neighbors (on average $\langle k \rangle - 1$ neighbors) are taken into account but the correlations between these neighbors are neglected. The equations of evolution involve the auxiliary

quantity:

$$\Theta^{nn}(t) = \left[1 - \frac{c_{SE}^{nn}}{c_{S}^{nn}(t)}\right] = \left[1 - \frac{c_{SE}^{nn}}{c_{SE}^{nn} + c_{SR}^{nn} + c_{SS}^{nn}}\right]. \tag{10}$$

Pair densities being symmetric (i.e., $c_{SE}^{nn} = c_{ES}^{nn}$), only six equations are required (cf. the corresponding formalism in [56]:

$$\begin{aligned}
c_{E,S}^{nn}(t+1) &= pc_{S,R}^{nn}(t)[f + (1-f)(1 - [\Theta^{nn}(t)]^{<k>-1})] \\
&+ (1-f)c_{S,S}^{nn}(t)[\Theta^{nn}]^{<k>-1} \\
&\quad [f + (1-f)(1 - [\Theta^{nn}]^{<k>-1})] \\
c_{E,R}^{nn}(t+1) &= c_{S,R}^{nn}(t)(1-p)[f + (1-f)(1 - [\Theta^{nn}]^{<k>-1})] \\
&+ c_{E,S}^{nn}(t)[f + (1-f)(1 - [\Theta^{nn}]^{<k>-1})] \\
c_{S,R}^{nn}(t+1) &= c_{S,R}^{nn}(t)(1-p)(1-f)[\Theta^{nn}]^{<k>-1} \\
&+ (1-p)pc_{R,R}^{nn}(t) + pc_{E,R}^{nn}(t)(1-f)[\Theta^{nn}]^{<k>-1}c_{E,S}(t) \\
c_{E,E}^{nn}(t+1) &= c_{S,S}^{nn}(t)[f + (1-f)(1 - [\Theta^{nn}]^{<k>-1})]^2 \\
c_{R,R}^{nn}(t+1) &= (1-p)^2 c_{R,R}(t) + 2(1-p)c_{E,R}(t) + c_{E,E}(t) \\
c_{S,S}^{nn}(t+1) &= p^2 c_{R,R}^{nn}(t) + 2p(1-f)[\Theta^{nn}]^{<k>-1}c_{S,R}^{nn}(t) \\
&+ (1-f)^2[\Theta^{nn}]^{2(<k>-1)}c_{S,S}^{nn}(t).
\end{aligned} \tag{11}$$

Adding these equations shows that the conservation of $c_{S,S}^{nn}(t) + c_{R,R}^{nn}(t) + c_{E,E}^{nn}(t) + 2c_{E,S}^{nn}(t) + 2c_{E,R}^{nn}(t) + 2c_{S,R}^{nn}(t)$ is ensured at any time t, equal to 1 if satisfied at time $t = 0$. The equation for $c_{E,R}(t + 1)$ (i.e. a connected pair of nodes in states (E, R) at time $t + 1$) contains three terms: the probability that (E, R) is reached from (S, R), the first one becoming spontaneously active and the other not recovering; the probability that (E, R) is reached from (S, R), the first one becoming excited due to its excited neighbors and the other not recovering; and the probability that (E, R) is reached from (S, E), the first one becoming active and the other entering the refractory state. Fig 2 illustrates these equations in the form of a transition graph among pair states. Each circle represents the state of two nodes and the arrows represent the change of states. The quantities *ES* and *EE* have been highlighted along with their corresponding mean-field equations, as the comparison with synchronization measures will be built around them.

Results

Relationship between the two types of synchronization

We investigated the general relationship between the two types of synchronization, namely logistics and physics synchronization, in particular which type of synchronization dominates in which region of parameter space $\{p, f\}$. We used the simple computational model of machine activity in a production network described in Methods. We first considered a Barabasi-Albert (BA) graph [57] graph with 100 nodes and m=3 (number of edges attached from each added node during graph generation). Fig 3 illustrates the different relationship between physics and logistics synchronization for two distinct parameter settings (both at high average setup time for machines, i.e., low recovery probability $p = 0.15$). Fig 3a shows that there exists a clear anti-correlation between logistics and physics synchronization at this low recovery probability and low rate of conflicts with other production tasks or alternative products

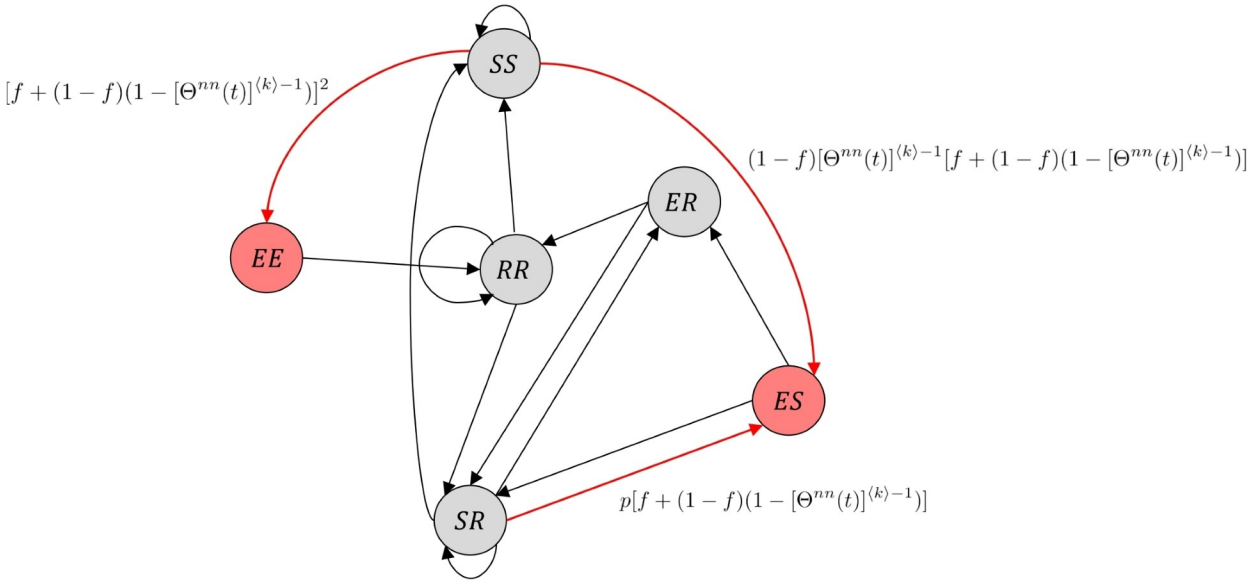

Fig 2. Evolution of pair densities resulting from pair-approximation (second-order) mean-field SER dynamics. Each circle represents a possible state of a pair of nodes and arrows represent state transitions. The cases ES and EE are emphasized with their evolution equations. The quantity $\Theta^{nn}(t)$ is given in Eq 10.

https://doi.org/10.1371/journal.pcsy.0000033.g002

(represented by spontaneous activation with rate f) ($p = 0.15, f = 0.001$). The results are drawn from running simulations on one BA network for 40 runs. The results also hold when we use different 100-node BA graphs for each run of SER dynamics (S2 Fig). This implies that activity organizes itself either into markedly synchronous or markedly sequential activity, but not both. However, when only increasing the rate of spontaneous activation ($f = 0.1$), the two types of synchronization become independent (zero correlation) or are slightly positively correlated

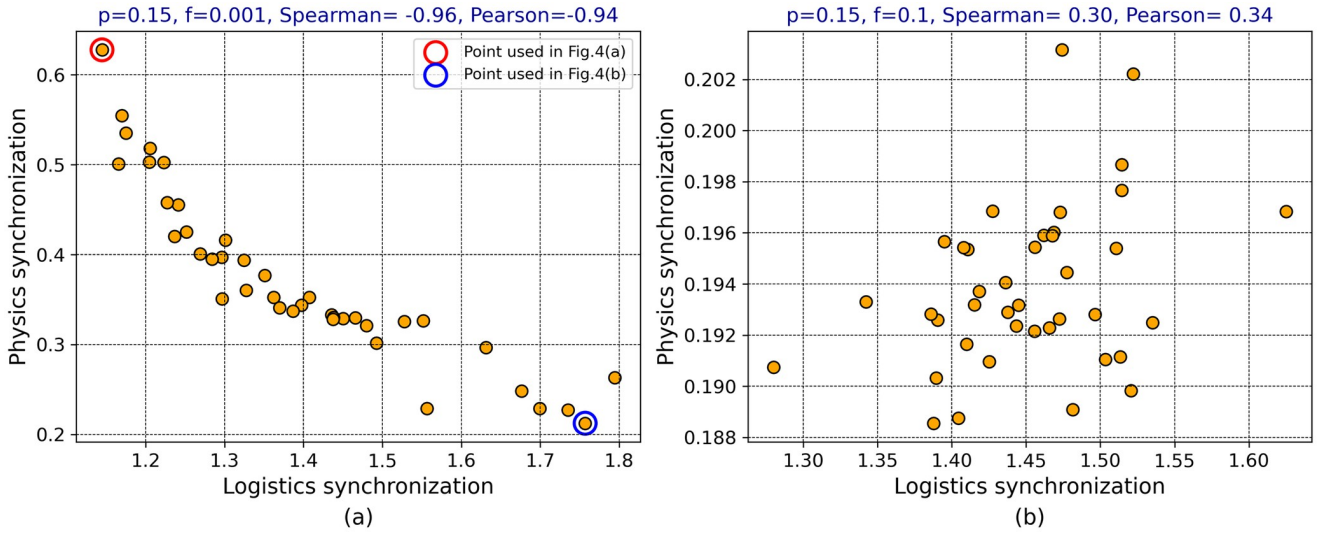

Fig 3. Scatter plots of physics synchronization and logistics synchronization. (a) Synchronization values observed for recovery probability $p = 0.15$ and rate of spontaneous activation $f = 0.001$. (b) Synchronization values for $p = 0.15$ and $f = 0.1$. Each point in the graph represents the value for one network realization of a 100 node BA graph with $m = 3$, the same network is used for all the 40 runs involved in the computation of synchronization measures.

https://doi.org/10.1371/journal.pcsy.0000033.g003

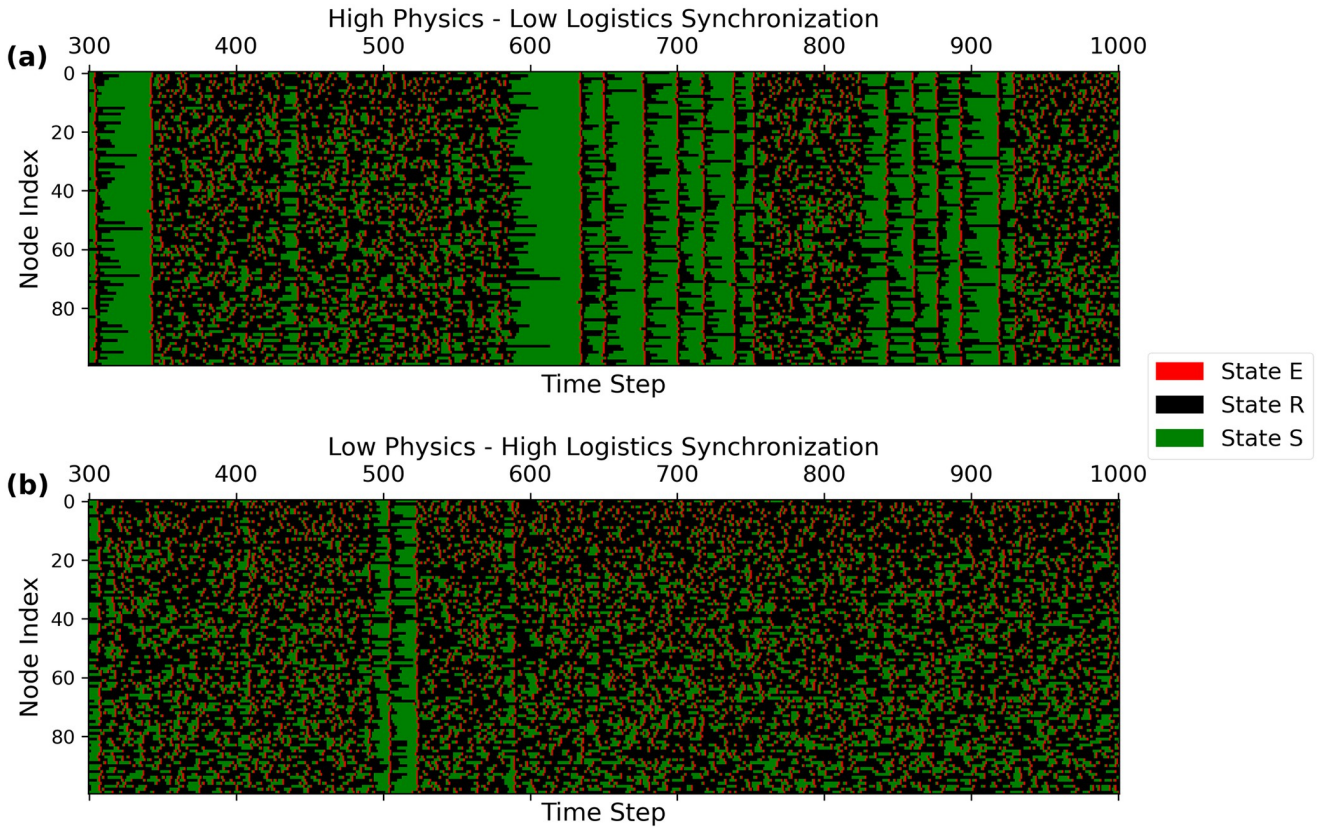

Fig 4. Space-time plot showing the state of the nodes (vertical axis) across time (horizontal axis) in a 1000 steps simulation of SER dynamics on a 100-node BA graph. (a) shows a realization for high physics and low logistics synchronization, whereas (b) shows a realization for a low physics and high logistics synchronization. The two panels illustrate two extreme situations originating from two different runs at fixed rate of spontaneous activation $f = 0.001$ and recovery probability $p = 0.15$. The first 300 time steps have been discarded as transient.

https://doi.org/10.1371/journal.pcsy.0000033.g004

as shown is Fig 3b, suggesting that the relationship between the two quantities indeed depends on the details of the activity regime.

When plotting the system state as a function of time across all nodes (arranged linearly in a random order), one can see the qualitative change in the pattern of activity. The two space-time plots Fig 4 display two extreme (and opposite) values of physics and logistics synchronization under the same parameter setting $p = 0.15$, $f = 0.001$ and different runs. The figure visually evidences that in case of high physics (parallel) and low logistics (sequential) synchronization values (Fig 4a), the system has prolonged areas of no activity during which it remains mostly susceptible, leading to greater value of co-activation in fixed intervals. On the other hand, in Fig 4b for low physics synchronization (bottom panel), we can see that activity level remains mostly stable (and high) across all time points, leading to greater sequential activation values.

For a further understanding, we simulated the dynamics for different recovery probabilities under different rates of spontaneous activation as presented in Fig 5, where the correlation coefficient between physics and logistics synchronization, denoted by r_{LP}, is shown. Looking at the correlation values for different values of recovery probabilities with respect to different rate of spontaneous activation f, some systematic trends in the relationship between the two quantities become discernible. For a lower value of spontaneous activation ($f = 0.001$) and higher values of recovery probability ($p = 0.3$ to 1.0), the range of values for the physics synchronization index across different runs becomes very narrow (see Fig 3b and S2 Fig). Physics

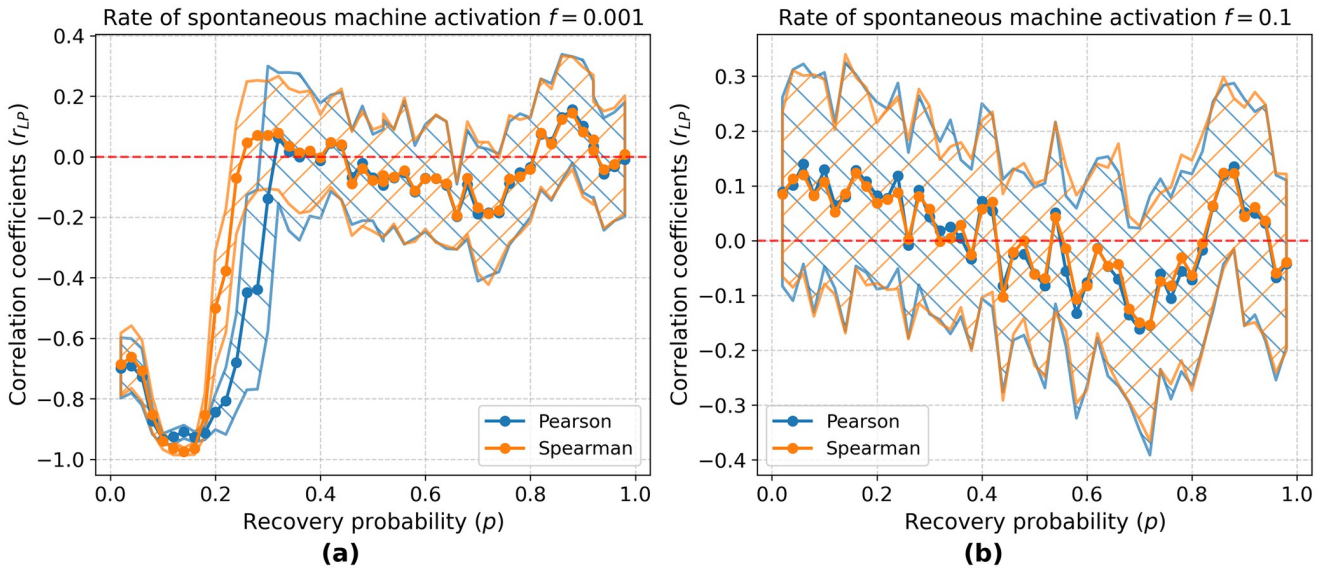

Fig 5. Correlation between logistics and physics synchronization as a function of recovery probability *p*. (a) shows the correlation for a low rate of spontaneous machine activation $f = 0.001$ (b) shows the correlation for a high rate of spontaneous machine activation $f = 0.1$. Pearson and Spearman correlations have been calculated from 40 runs of SER dynamics on the same BA graph with 100 nodes and m=3. The mean and standard deviation (hatched zones) has then been calculated by repeating the same experiment 30 times.

https://doi.org/10.1371/journal.pcsy.0000033.g005

synchronization is there coincidental, and the observed synchronization level depends only on the activity level in the network, which is roughly identical across different runs at fixed p and f. The residual fluctuations within this narrow range are indicative of a small residual flexibility in the excitation distribution (nodes in state E) at a given activity level. In this way, there is enough stochasticity to compute a non-trivial (non vanishing) correlation. This correlation takes a weak positive value.

Our simulation results show that random spontaneous activation with rate f, representing disruptions of the standard production plan, indeed changes the relationship between the two types of synchronization in a qualitative fashion, i.e. from a negative (either/or) relationship at low f (low disruption level) to independence at high f (high disruption level). These transitions have been better realized in the form of a heatmap (Fig 6), where the transition of negative correlation to uncorrelated/ weak positive correlation can be clearly seen for different values of f. Based on the changes in the two types of synchronization with the parameters of the SER model and the information contained in the space-time plots on Fig 4, we can summarize our physical intuition about these processes as follows: With increasing p the dynamics undergo a transition from perpetually re-initialized dynamics via spontaneous activation (from a network state where all nodes are in S state) to self-sustained activity. This transition has been studied in the SER model before [58–60]. Re-initialized dynamics result in high physics synchronization: synchronous groups of nodes due to distance from a random excitation triggering a wave of activity in the system. Self-sustained activity results in high logistics synchronization: many local wave fronts meandering through the system without interfering and thus contributing to a strong enhancement of sequential activation along the edges of the graph. At low p an increase in f can trigger a similar multi-wavefront pattern and hence a transition from high physics to high logistics synchronization.

A key insight in the interpretation of logistics synchronization is its association with the presence of collective, self-organized activity waves in the network. We have quantitatively

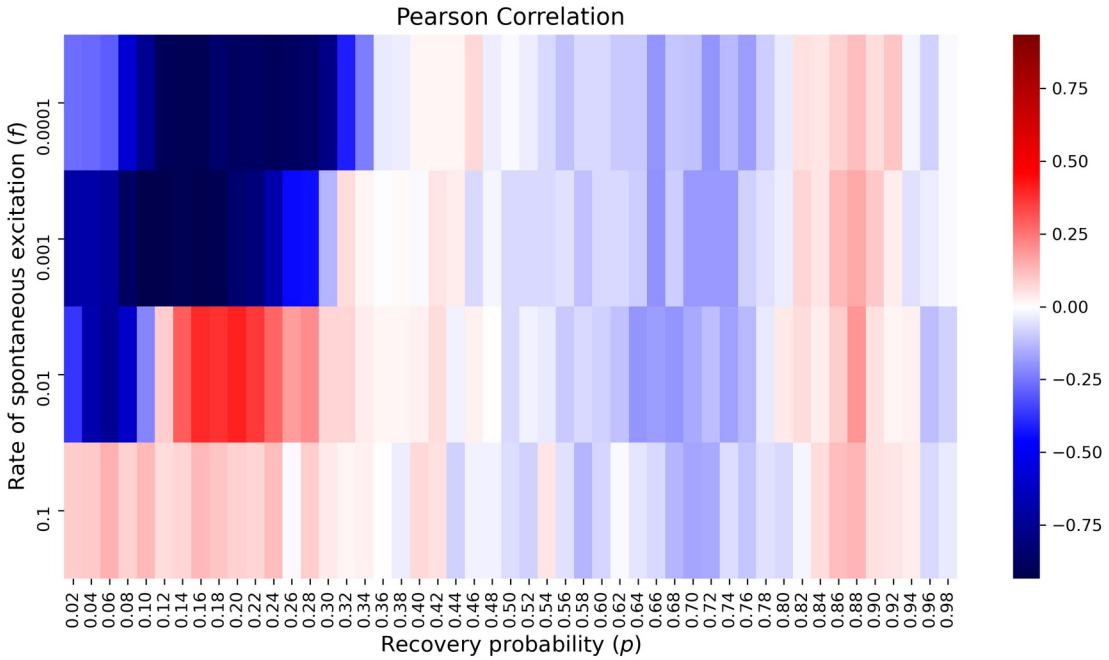

Fig 6. A heatmap showing the correlation between logistics and physics synchronization across a range of values of *p* and four values of *f*. The transition of negative correlation to uncorrelated/weak positive correlation can be clearly seen for the different values of *f*. The network used is a BA graph with 100 nodes and $m = 3$. Pearson correlation has been computed from 40 individual runs on the same network realization, followed by averaging over 30 such numerical experiments.

https://doi.org/10.1371/journal.pcsy.0000033.g006

assessed this association using a method introduced in [61]. It involves the auxiliary notion of link usage asymmetry, defined as the bias, at a link of the graph, of excitation propagating in one direction and in the other direction. The presence of wave patterns propagating from a hub is then evidenced as the alignment of the link usage asymmetries with the orientation of a link to the set of nodes with the highest degree, called hub-set orientation prevalence in [61]. Wave pattern strength is simply measured as the Pearson correlation coefficient between these two quantities. The scatterplot of logistics synchronization against wave pattern strength displayed in Fig 7 shows a clear positive correlation. So, indeed, high logistics synchronization goes along with stronger self-organized excitation waves in the graph.

Influence of network architecture

In this section we explore the synchronization patterns arising in different network architectures with respect to the parameters *p* and *f*. In S2 and S3 Figs the physics and logistics synchronization measures are studied individually as a function of the parameters (*p* and *f*). For our study we use BA and ER graphs as representations of two extremes in production network architectures: In ER graphs [62] all nodes have very similar degrees, while in BA graphs the process is centered around a few high-degree nodes, the hubs of the production system. These basic models have been used quite widely in the study of production systems ([63–65]) and are introduced in S1 Appendix. S3 Fig presents our results for BA [57] graph. We observe that the region of very low *p* shows a markedly different behavior. This is less pronounced the larger the network is, and stronger in BA graphs than in ER graphs. As production networks are often not very large (they are often on the scale of a few tens to a few hundreds of nodes) such effects can be important in realistic settings. S4 Fig represents our results for an ER graph

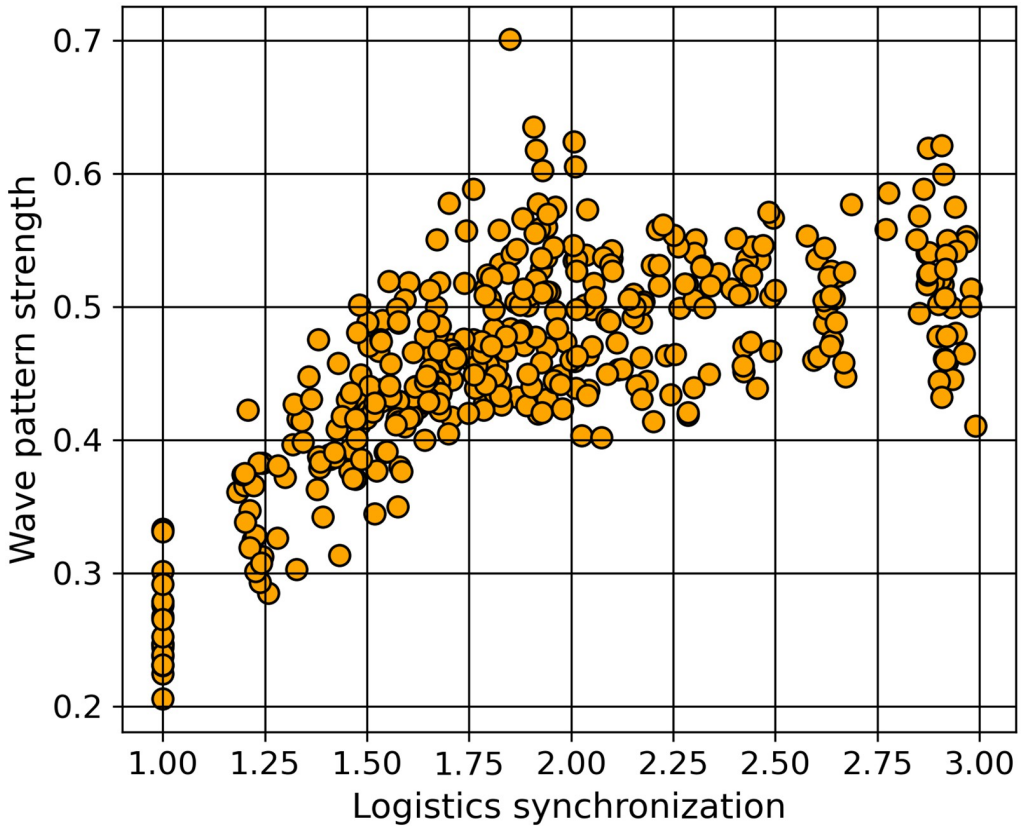

Fig 7. Scatterplot of logistics synchronization and wave pattern strength. Time series of 5000 steps have been simulated on 20 different BA graphs (number of nodes $N = 100$, connection parameter $m = 5$) for $f = 0.005$ and p ranging from 0.05 to 1 (varied in steps of 0.05). Wave pattern strength has been computed according to [61] with a hub set size of $N/2$. The correlation coefficient between logistics synchronization and wave pattern strength is 0.66.

https://doi.org/10.1371/journal.pcsy.0000033.g007

which are in very close agreement with the results from BA graph. The two types of synchronization deviate from the general trend in a highly sensitive parameter space region, corresponding to low machine recovery probability ($p \leq 0.2$) and low rate of spontaneous machine activation (f).

In several recent investigations it has been studied, how co-activation (the main driver of physics synchronization) and sequential activation (the mechanism underlying logistics synchronization) are changing as a function of network architecture and the dynamical processes at work. While there is no all-encompassing theory relating these two quantities, a few general principles have emerged: On a local scale and near the deterministic limit of the dynamics, the topological overlap (i.e., the normalized number of common neighbors of two nodes) is determining co-activation ([66]). Across a range of dynamics, the agreement between structural connectivity and co-activation patterns (SC/FCc) vs. sequential activation patterns (SC/FCs) tends to behave antagonistically: if one is high, the other is low [55]. BA graphs tend to have strong (SC/FCs), while ER graphs tend to have stronger (SC/FCc) [60]. Co-activation and sequential activation are obviously pairwise approximations of the actual levels of synchronization in the system. We can resort to the mean-field analysis described above to assess, how well these 'local proxies' describe the two types of synchronization.

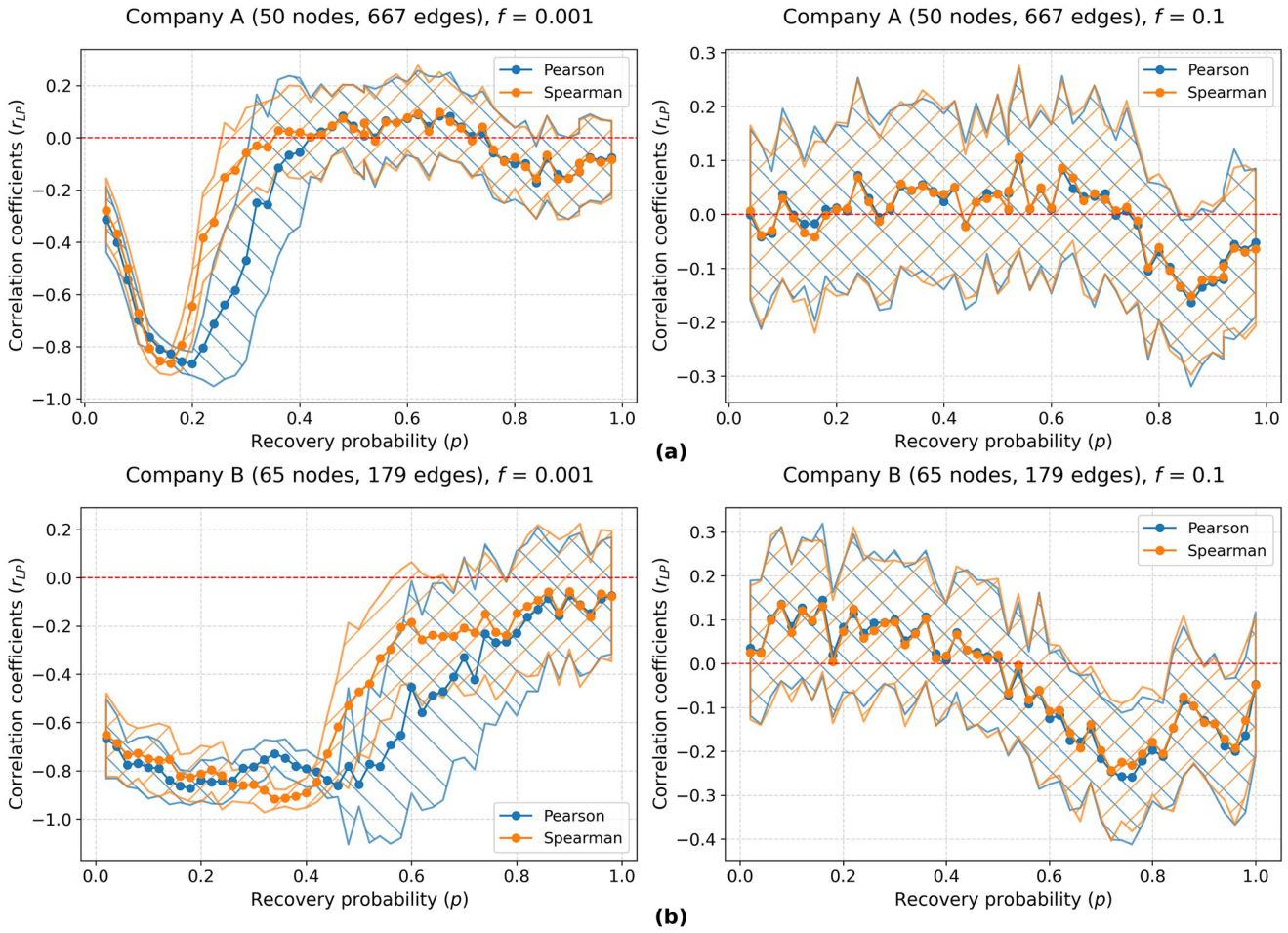

Fig 8. Correlation between logistics and physics synchronization as a function of recovery probability p in real production networks. (a) company A network (b) company B network for low spontaneous machine activation rate $f = 0.001$ (left) and high rate of spontaneous machine activation rate $f = 0.1$. (right). The mean and standard deviation (hatched zones) has then been calculated by repeating the same experiment 30 times. Note that the range can end slightly below −1 in some cases due to the definition of the hatched zone (mean ± standard deviation).

https://doi.org/10.1371/journal.pcsy.0000033.g008

Application to real data

Our synchronization study has been carried out on real-life production network using datasets from two manufacturing companies named as Company A and Company B. Company A has 50 nodes, 667 edges while Company B has 65 nodes and 179 edges. These companies have already been part of the set of networks studied in [47] which helps in transferring our hypothesis from synthetic models to real world production networks and thus strengthening our findings. Fig 8 shows our findings on these real production networks. A shift from high negative correlation (between physics and logistics synchronization) to weak correlations is seen in across values of recovery probability p for $f = 0.001$, similar to our findings on synthetic models.

Mean-field analysis results

Comparing mean-field predictions with numerical results provide a mechanistic insight of which features and patterns of the dynamics can, or cannot, be explained by taking into account pairwise correlations alone, following the methodology presented in [56]. In our

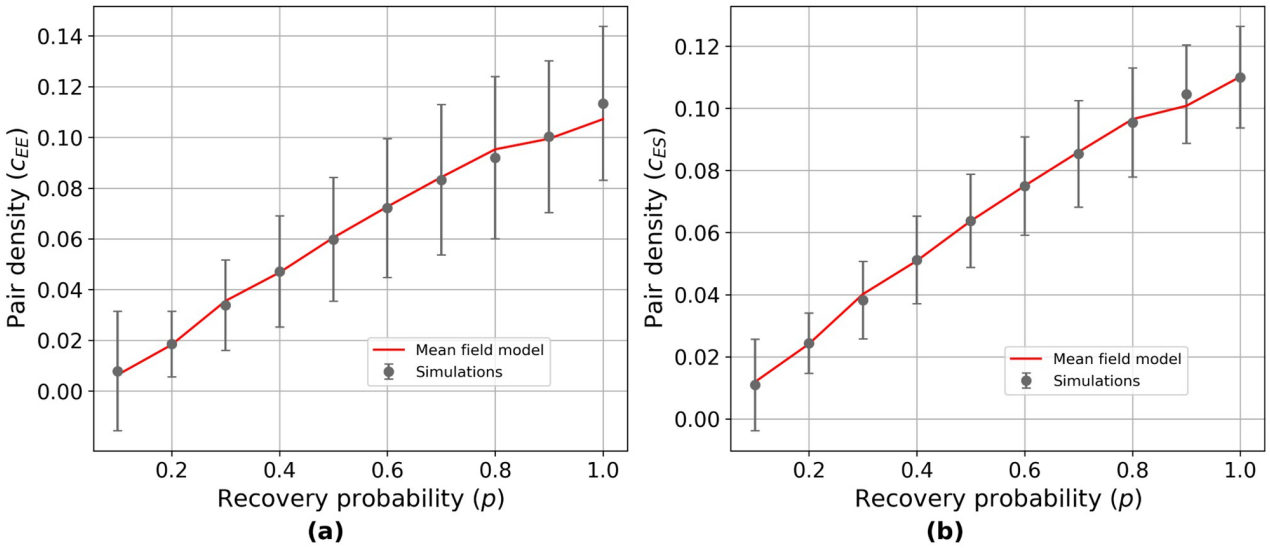

Fig 9. Value of pair densities. (a) $c_{E,E}$ (b) $c_{E,S}$ obtained in the simulation, and the steady-state solution of mean-field Eq 11 (given in red) for varying values of the recovery probability p. Error bars on simulation points have been obtained from the last 500 time steps of a 1000 time-step simulation starting from random initial conditions.

https://doi.org/10.1371/journal.pcsy.0000033.g009

simulations, the initial condition has been taken at random, with equal fractions of susceptible (S), excited (E) and refractory (R) nodes spanning the graph. A highly connected ER graph with 100 nodes and 500 edges with recovery probability p=0.3 and rate of spontaneous activation f=0.01, is used. All the spatio-temporal correlations and network heterogeneities are by construction taken into account in the simulation. We here present the investigation for pair densities $c_{E,E}$ and $c_{E,S}$. S5 Fig shows a simulated time course of these two pair densities (after discarding initial transients) as well as a moving average. The simulated densities lies around the stationary-state mean-field prediction, with some slight fluctuations of relatively low amplitude. The comparison of the numerically simulated stationary state and its mean-field prediction is presented in Fig 9 for various values of the recovery probability p and a rate of spontaneous activation f=0.01. Fig 9a shows that pair-approximation mean-field equations are successful in predicting the co-activation of nodes as described by the pair density $c_{E,E}$, while Fig 9b shows the same agreement for sequential activity in the network, as described by the pair density $c_{E,S}$. This agreement supports that pair correlations between neighboring machines fully determine these pairwise quantities.

Proxies for the two types of synchronization

In the previous section, the numerical implementation of the SER model displayed a shift from positive to negative correlation between logistics and physics synchronization when dynamic parameters p and f vary. The mean-field analysis now offers the possibility to identify mean-field representations ('proxies') of the synchronization measures.

(i) Logistics synchronization. As defined in the previous section, logistics synchronization is sensitive to the flow of activity from one machine to another in a production network. It is therefore natural to associate logistics synchronization with the pair density $c_{E,S}$:

$$\sigma_L \sim c_{E,S}, \tag{12}$$

where σ_L is the logistics synchronization index and $c_{E,S}$ the probability that in a pair of neighbors, the first node is excited (state E) and the other is in the susceptible state S.

(ii) Physics synchronization. Physics synchronization is related to the co-activation of machines in the system. It is thus natural to associate physics synchronization with the pair density $c_{E,E}$:

$$\sigma_P \sim c_{E,E}, \tag{13}$$

where σ_P is the physics synchronization index, $c_{E,E}$ denotes the probability that in a pair of neighbors, both nodes are simultaneously excited (state E).

To explore how well these mean-field proxies give access to the actual synchronization behavior, we run the simulation on two different kinds of graphs, ER random graphs and BA scale-free graphs, and the logistics and physics synchronization measures are compared with their respective mean-field proxies.

S6 Fig shows that the proxy $c_{E,E}$ is positively correlated with physics synchronization measure σ_P for the vast range of recovery probability $p = 0.2$ to 1.0, while it differs for the lower range $p = 0.02$ to 0.1. S7 Fig shows that the proxy $c_{E,S}$ is positively correlated with logistics synchronization for lower values of recovery probability p, while for higher values the relationship shifts towards an anti-correlation. The discrepancy between mean-field proxies and simulated synchronization measures is more marked for BA graphs, as expected since the wide degree distribution of BA graphs is not consistent with the mean-field approximation of spatial homogeneity, in particular replacing the degree of each node with the average degree $\langle k \rangle$.

In conclusion, mean-field proxies for synchronization measures display a discrepancy with the numerical implementation of the SER dynamics, showing that higher-order correlations and spatial inhomogeneities are centrally involved in the synchronization behavior at low values of the recovery probability ($p < 0.2$). These insights agree with our physical understanding: determinant spatial inhomogeneities are typically a center node from which a wave of activity is triggered (in particular in re-initialized dynamics from a network state with all nodes in state S) while higher-order correlations (i.e. involving more than two nodes, in clusters or along paths of the network) are determinant in self-sustained activity.

Robustness

As a final step, we briefly explored the relationship between synchronization measures and performance indicators. A well-functioning production network has to fulfill the product demand or jobs at the correct time. Quality is measured using key performance indicators, or KPIs, which demonstrate the flexibility, stability, agility of a production system. As an example, we here set out to define and understand the systematic relationship between the flow- and the system- oriented notion of synchronization, i.e. logistics and physics synchronization, and its relation to robustness.

Robustness of a network can be defined as the ability of the system to maintain its functionality and performance despite the fact the a part of the network has been damaged due to random disruption or attacks [67]. Attacks on a system can be either be *natural* attacks or *targeted* attacks which could disrupt the functioning of the system. An example of these two kinds of attacks can be explained with respect to a car production factory. A natural failure occurs, when a job shop fails to produce the required part of a car leading to delayed production, while a targeted attack can be explained as an attack on the key software by enemies to hack into the system causing breakdown. For the scope of this study, we have considered attacks or disruptions to be only natural in nature to express them in our minimal model of machine

activity two primary mechanisms can be used: we can use removal of nodes or removal of edges to replicate breakdown of flow in a production system. Here for our investigation we have used the latter. A simple representation of performance is to compute the average change in machine activity under removal of an edge. A deletion of an edge represents a disruption in machine network, i.e. machine activity at one edge will not trigger activity at the other. Average excitation change can thus serve as a performance indicator of synchronized production systems since it shows the system's response to disruptions. In our simple model, high changes in average machine activity under link deletion suggest that the activity pattern is not structurally robust and hence indicative of systemic vulnerability. We numerically observe that synchronization can serve as an indicator of such vulnerability, with high logistics synchronization being associated with smaller change in average excitation density, while under certain parameter conditions physics synchronization being associated with higher average change. By monitoring synchronization, we can thus estimate the robustness of the overall system. A more detailed mechanistic understanding of this relationship would require more refined models of machine activity. The impact of edge deletion on machine activity will strongly depend on the precise position of the edge in the network (see [68–70], as examples of edge importance studies). As we are rather interested in global effects, we average over all edges in the graph and compare this average change in activity in a network with average change in synchronization measures accompanying it. In our analysis we have taken 40 ER graphs and ran the SER dynamics on them. Simultaneously we have used the mechanism of edge removal and systematically deleted every edge (one at a time) such that at every point in time the graph has one edge missing. Then we have computed for each graph (1) logistics synchronization, (2) physics synchronization, (3) excitation density for the unperturbed graph and (4) the average excitation density under removal of a single edge. In this way we can compare the average change in excitation density upon edge removal with both types of synchronization. The experiment is then conducted across 30 runs and we then plot the correlations between the average excitation change and logistics synchronization (represented by r_{EL}) as well as physics synchronization and average excitation change (represented by r_{EP}) for varying recovery probabilities and machine activity. Fig 10 summarizes the results of this numerical experiment over a wide range of machine recovery probability p and two values of random spontaneous machine activation $f = 0.001, 0.1$ respectively.

The first plots of Fig 10 respectively (left) shows that for low recovery probability (p=0.1) and low rate of spontaneous machine activation (f=0.001), change in excitation density matches both logistics and physics synchronization, which suggests that higher logistics synchronization is associated with a more stable and resilient systems. When physics synchronization increases so does average excitation change suggesting the system's sensitivity to network changes. On increasing the value of recovery probability p, the change in excitation densities matches only physics synchronization. In case of a high rate of spontaneous machine activation ($f = 0.1$), even for small recovery probabilities average excitation change is no longer governed by logistics synchronization. Physics synchronization exhibits a negative relationship with average excitation change for higher values of recovery probability irrespective of the rate of machine activity.

Conclusion and outlook

In this study we have shown that there exists a dual parameter-dependent relationship between logistics and physics synchronization. The results show a shift from positive to negative correlation between the two types of synchronization as a function of production settings, which can be exploited in monitoring the production systems.

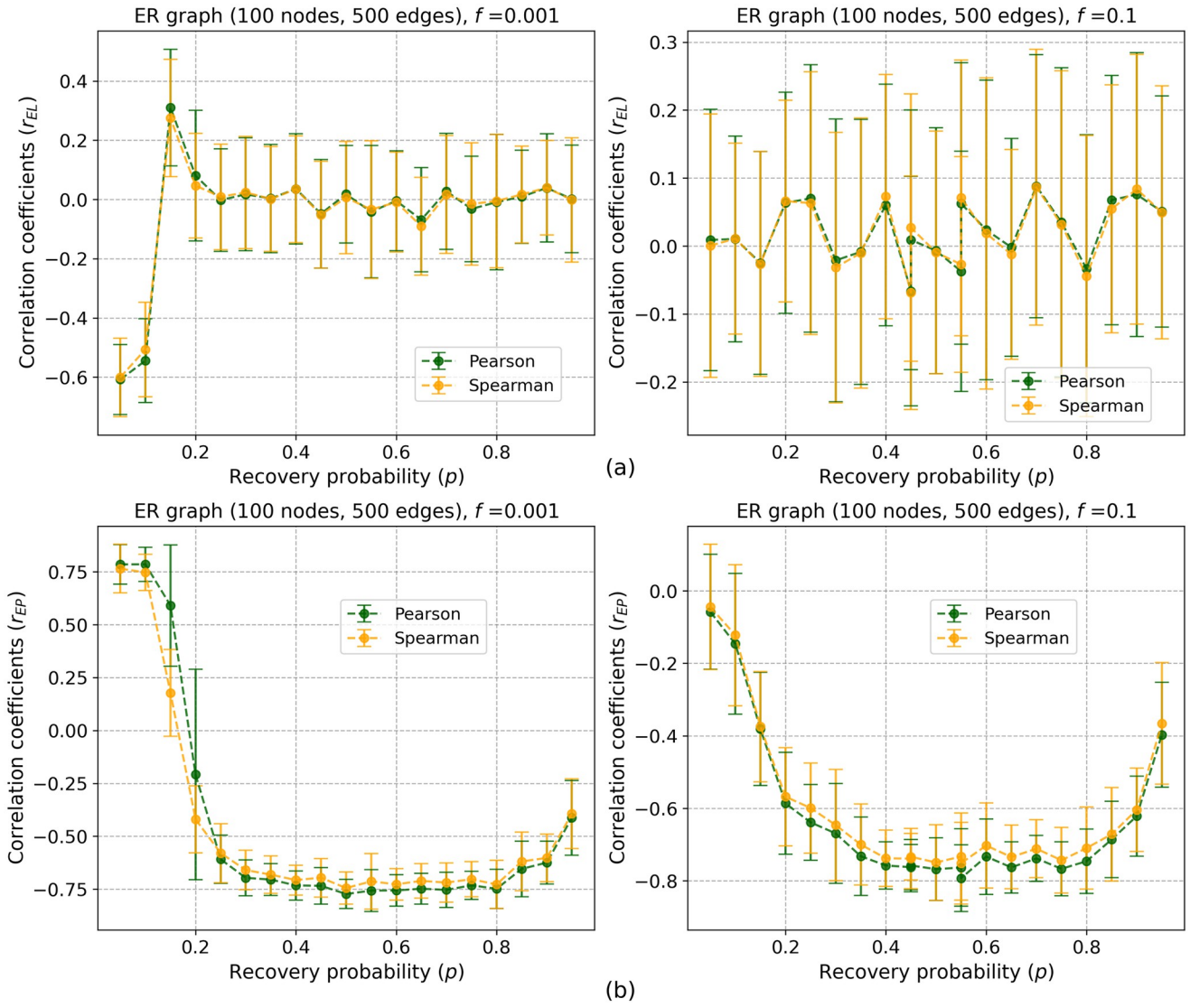

Fig 10. Correlations between average excitation change upon edge removal and synchronization measures. (a) Correlation r_{EL} between average excitation change and logistics synchronization for rate of machine activation f=0.001 (left) and f = 0.1. (right) (b) Correlation r_{EP} between average excitation change and physics synchronization for rate of spontaneous machine activation f=0.001 (left) and f = 0.1 (right). Simulations have been performed on an ER graph with 100 nodes and 500 edges for varying values of the recovery probability p. Error bars on simulation points have been obtained from 50 runs for each type of correlation (Pearson or Spearman).

https://doi.org/10.1371/journal.pcsy.0000033.g010

The two extreme cases of network architectures studied here, scale-free graphs (BA graph) and random graphs (ER graph), are both quite similar in the relationship between physics and logistics synchronization when the two parameters of the model are varied. This suggest that structural differences like bottlenecks (hubs) through which a huge number of production steps run) and more distributed production networks, where all machines have essentially the same level of specialization and task distribution (nodes all having a similar degree in the corresponding network abstraction) do not qualitatively affect synchronization behavior. The only difference between these network architectures is the higher sensitivity to spontaneous activation in BA graphs compared to ER graphs in the low-p regime.

Our investigation furthermore points to the importance of latency time distributions (in our model governed by the recovery probability p). An increase in p leads to an increase in the positive correlation value between logistics and physics synchronization. A mean-field analysis of the dynamic model has helped to understand the two types of synchronization more deeply. Mean-field solution agrees with numerical results for pair densities, showing the mechanistic origin of their value in pairwise correlations between neighboring machines. In contrast, mean-field proxies for synchronization measures display a discrepancy with simulations, showing that higher-order correlations and spatial inhomogeneities are centrally involved in the synchronization behavior. This insight agrees with our physical understanding: determinant spatial inhomogeneities are typically a center node from which a wave of activity is triggered, while higher-order correlations (i.e. involving more than two nodes) are determinant in self-sustained activity.

For industrial practice, our results offer indicators how activity patterns are affected by the design of the production network as well as its planning and control. Though using directed graphs would align more closely with the real, sequential nature of production and logistics processes, undirected graphs can effectively model production and logistics networks too by capturing mutual dependencies and simplifying system-wide analyses of connectivity and robustness. It allows a view of synchronization and coordination, particularly useful for systems that prioritize timing over strict flow direction and offer a streamlined representation for early-stage planning and structural insights. Thus, our minimal model can be used to pursue a range of further research questions: (1) The sequential activation matrix asymmetry [61] can be an indicator of the establishment of waves and perhaps even the establishment of well-defined paths through the system, which could indicate the emergence of a product portfolio. (2) In our study, we have considered the overall logistics synchronization of a system. However, considering it as a function of individual nodes (machines) would help understand vulnerabilities at production paths. In general, path selection heuristics and product portfolio diversity can prove to be new avenues of graph-theoretical methods in industrial production.

The phenomenon of synchronization in a minimal model of machine activity can further be developed to incorporate more key performance indicators (KPIs) of the system. We here have studied only the effect of synchronization on one such key performance indicator, i.e., robustness. Simulation studies concentrating on recording excitation frequencies of the nodes could be used to systematically include idle time in the study. A higher excitation density of nodes in a stylized version could represent minimized idle time of machines. Also, the effect of synchronization on input-output correlations could suggest the capacity of the system to enhance the due date reliability of the system. The study uses a stylized version of a production process. The dynamic rule governing the states of nodes relies on the foundation that every machine available for work (susceptible) goes into the excited state to process the order. However the model does not take into account the probability of machine failure i.e. it doesn't account for the case in which the machine available for a job breaks down and again enters the maintenance (refractory) state. In our further studies we would like to include machine failure probability p_R and study the general trends of synchronization in such a setting.

Another aspect worthwhile to pursue is the comparison with discrete event simulation (DES) which is frequently used to study manufacturing systems. The DES results can be used directly to validate the results from the minimal model described here on the relationships between the various types of synchronization and logistics performance indicators. In combination, the minimal model results and a future DES validation will form the basis for a mechanistic understanding of the interplay between function and emergence of synchronization in manufacturing systems.

Supporting information

S1 Appendix. Definition of BA and ER graphs.
(PDF)

S1 Fig. State transitions in the SER model and the standard (first-order) mean-field expressions governing them, with $\theta(t) = [1 - c_E(t)]$.
(PDF)

S2 Fig. Scatter plots of physics synchronization and logistics synchronization. Synchronization values observed for recovery probability $p = 0.15$ and rate of spontaneous activation $f = 0.001$. Each point in the graph represents the value for one network realization of a 100 node BA graph with $m = 3$, different networks have been used for 40 runs involved in the computation of synchronization measures.
(PDF)

S3 Fig. Logistics and physics synchronization measures σ_L and σ_P as a function of the recovery probability p in a BA graph. The network is a BA graph with 100 nodes and 291 edges, and p is varied from 0.05 to 1.0 with steps of 0.05. The rate of spontaneous activation f was fixed, and three different values 0.001, 0.01, 0.1 have been considered. The mean and standard deviation (hatched zones) have been calculated by repeating the same experiment 30 times.
(PDF)

S4 Fig. Logistics and physics synchronization measures σ_L and σ_P as a function of the recovery probability p in an ER graph. The network contains 100 nodes and 500 edges, where p is varied from 0.05 to 1.0 with steps of 0.05. The rate of spontaneous activation f has three different values 0.001, 0.01, 0.1. The mean and standard deviation (hatched zones) have been calculated by repeating the same experiment 30 times.
(PDF)

S5 Fig. Mean-field pair densities c_{ES}, c_{EE} and their simulated counterparts on a connected random graph. Simulation has been performed with a spontaneous activation rate $f = 0.01$, a recovery probability $p = 0.3$, on a random graph (Erdős-Rényi) with 100 nodes and 500 edges. The figure displays the simulated time course of the pair density (highly fluctuating orange line), its moving average (blue curve) and the steady-state solution of mean-field equations in red. The time window of the moving average is two.
(PDF)

S6 Fig. Physics synchronization vs. its mean-field proxy. Comparison between physics synchronization and $c_{E,E}$ for (a) an ER graph (b) a BA graph. Each point on the graph represents one network realization of a single value of recovery probability p, where p ranges from 0 to 1 in steps of 0.02. The rate of spontaneous excitation is $f = 0.001$. The dashed line facilitates reading by connecting the values for ascending values of p.
(PDF)

S7 Fig. Logistics synchronization vs. its mean-field proxy. Comparison between logistics synchronization and $c_{E,S}$ in (a) an ER graph (b) a BA graph. Each point on the graph represents one network realization of a single value of recovery probability p, where p ranges from 0 to 1 in steps of 0.02. The rate of spontaneous excitation is $f = 0.001$. The dashed line facilitates reading by connecting the values for ascending values of p.
(PDF)

S1 Video. SER dynamics on a BA graph with recovery probability $p = 0.1$ and rate of spontaneous machine activation $f = 0.001$.
(MP4)

S2 Video. SER dynamics on a BA graph with recovery probability $p = 0.8$ and rate of spontaneous machine activation $f = 0.001$.
(MP4)

S3 Video. SER dynamics on a BA graph with recovery probability $p = 0.1$ and rate of spontaneous machine activation $f = 0.1$.
(MP4)

S4 Video. SER dynamics on a BA graph with recovery probability $p = 0.8$ and rate of spontaneous machine activation $f = 0.1$.
(MP4)

Author Contributions

Conceptualization: Sanghita Bose, Annick Lesne, Marc-Thorsten Hütt.

Data curation: Sanghita Bose.

Formal analysis: Sanghita Bose, Annick Lesne, Marc-Thorsten Hütt.

Funding acquisition: Julia Arlinghaus, Marc-Thorsten Hütt.

Investigation: Sanghita Bose, Annick Lesne.

Methodology: Sanghita Bose, Marc-Thorsten Hütt.

Project administration: Marc-Thorsten Hütt.

Resources: Julia Arlinghaus, Marc-Thorsten Hütt.

Software: Sanghita Bose.

Supervision: Annick Lesne, Julia Arlinghaus, Marc-Thorsten Hütt.

Validation: Annick Lesne, Julia Arlinghaus, Marc-Thorsten Hütt.

Visualization: Sanghita Bose, Marc-Thorsten Hütt.

Writing – original draft: Sanghita Bose, Annick Lesne, Julia Arlinghaus, Marc-Thorsten Hütt.

Writing – review & editing: Sanghita Bose, Annick Lesne, Julia Arlinghaus, Marc-Thorsten Hütt.

References

1. Winfree AT. Biological rhythms and the behavior of populations of coupled oscillators. Journal of theoretical biology. 1967; 16(1):15–42. https://doi.org/10.1016/0022-5193(67)90051-3 PMID: 6035757
2. Kuramoto Y. Chemical Oscillations, Waves, and Turbulence. Berlin: Springer; 1984.
3. Strogatz SH. From Kuramoto to Crawford: exploring the onset of synchronization in populations of coupled oscillators. Physica D: Nonlinear Phenomena. 2000; 143(1-4):1–20. https://doi.org/10.1016/S0167-2789(00)00094-4
4. Strogatz SH. Sync: How Order Emerges From Chaos In the Universe, Nature, and Daily Life. New York: Hyperion Books; 2003.
5. Pikovsky A, Rosenblum M, Kurths J. Synchronization: A Universal Concept in Nonlinear Sciences. vol. 45. Cambridge: Cambridge University Press; 2003.

6. Osipov GV, Kurths J, Zhou C. Synchronization in Oscillatory Networks. Berlin: Springer; 2007. Available from: http://www.springer.com/physics/complexity/book/978-3-540-71268-8.
7. Mikhailov AS, Calenbuhr V. From cells to societies: models of complex coherent action. Springer; 2002.
8. Haken H. Synergetics: An introduction. Nonequilibrium Phase Transitions and Self-Organization in Physics. Berlin: Springer; 1977.
9. Rodrigues FA, Peron TKD, Ji P, Kurths J. The Kuramoto model in complex networks. Physics Reports. 2016; 610:1–98. https://doi.org/10.1016/j.physrep.2015.10.008
10. Menck PJ, Heitzig J, Kurths J, Schellnhuber HJ. How dead ends undermine power grid stability. Nature communications. 2014; 5. https://doi.org/10.1038/ncomms4969 PMID: 24910217
11. Motter AE, Myers SA, Anghel M, Nishikawa T. Spontaneous synchrony in power-grid networks. Nature Physics. 2013; 9(3):191–197. https://doi.org/10.1038/nphys2535
12. Nyhuis P, Wiendahl HP. Fundamentals of Production Logistics: Theory, Tools and Applications. Engineering online library. Berlin, Heidelberg: Springer; 2008. Available from: https://books.google.com/books?id=dSz2-1KQcOkC.
13. Narahari Y, Viswanadham N, Bhattacharya R. Design of synchronized supply chains: A six sigma tolerancing approach. In: Robotics and Automation, 2000. Proceedings. ICRA'00. IEEE International Conference on. vol. 2. IEEE. San Francisco, CA: IEEE; 2000. p. 1151–1156.
14. Miller WA, Davis RP. Synchronization of material flow to aid production planning in a job shop. Engineering Management International. 1989; 5(3):179–184. https://doi.org/10.1016/S0167-5419(89)80015-8
15. Hoque Ma, Kingsman BG. Synchronization in common cycle lot size scheduling for a multi-product serial supply chain. International Journal of Production Economics. 2006; 103(1):316–331. https://doi.org/10.1016/j.ijpe.2005.08.007
16. Fernandes NO., Thürer M, Stevenson M, and Carmo-Silva S. (2020). Lot synchronization in make-to-order shops with order release control: an assessment by simulation. International Journal of Production Research, 2020; 58(21):6724–6738. https://doi.org/10.1080/00207543.2019.1685701
17. Guo D, Lyu Z, Wu W, Zhong RY, Rong Y, and Huang GQ. Synchronization of production and delivery with time windows in fixed-position assembly islands under graduation intelligent manufacturing system. Robotics and Computer-Integrated Manufacturing. 2022; 73:102236. https://doi.org/10.1016/j.rcim.2021.102236
18. Klug F. Synchronization transitions in supply chain networks. *International Journal of Systems Science: Operations & Logistics*, 2023; 10(1):2224104. https://doi.org/10.1080/23302674.2023.2224104
19. Chen J, Wang M, Kong XT, Huang GQ, Dai Q, and Shi G. Manufacturing synchronization in a hybrid flowshop with dynamic order arrivals. Journal of Intelligent Manufacturing. 2019; 30:2659–2668. https://doi.org/10.1007/s10845-017-1295-5
20. Pettersen J. Defining lean production: some conceptual and practical issues. The TQM Journal. 2009; 21(2):127–142. https://doi.org/10.1108/17542730910938137
21. Takeda H. The Synchronized Production System: Going Beyond Just-In-Time Through Kaizen. London: Kogan Page Publishers; 2006. Available from: http://books.google.com/books?id=bbILfqjKUMMC&pgis=1.
22. Coleman J, Lyons A, Kehoe D. The glass pipeline: increasing supply chain synchronisation through information transparency. International Journal of Technology Management. 2004; 28(2):172–190. https://doi.org/10.1504/IJTM.2004.005060
23. Doran D. Manufacturing for synchronous supply: a case study of Ikeda Hoover Ltd. Integrated Manufacturing Systems. 2002; 13(1):18–24. https://doi.org/10.1108/09576060210411477
24. Battini D, Boysen N, Emde S. Just-in-Time supermarkets for part supply in the automobile industry. Journal of Management Control. 2013; 24(2):209–217. https://doi.org/10.1007/s00187-012-0154-y
25. Hüttmeir A, De Treville S, Van Ackere A, Monnier L, Prenninger J. Trading off between heijunka and just-in-sequence. International Journal of Production Economics. 2009; 118(2):501—507. https://doi.org/10.1016/j.ijpe.2008.12.014
26. Scholl A. Balancing and sequencing of assembly lines. Heidelberg: Physica; 1996. Available from: http://books.google.de/books/about/Balancing_and_sequencing_of_assembly_lin.html?id=7PdTAAAAMAAJ&redir_esc=y.
27. Ohno T. Toyota Production System: Beyond Large-Scale Production. Portland, OR: Productivity Press; 1988. Available from: http://books.google.com/books?hl=en&lr=&id=7_-67SshOy8C&pgis=1.
28. Ali RM, Deif AM. Dynamic lean assessment for takt time implementation. Procedia CIRP. 2014; 17:577–581. https://doi.org/10.1016/j.procir.2014.01.128

29. Mueller A, Strzelczak S. Negative side effects of lean management. In: IFIP International Conference on Advances in Production Management Systems. Springer; 2014. p. 167–174.

30. Lindau RA, Lumsden KR. Actions taken to prevent the propagation of disturbances in manufacturing systems. International Journal of Production Economics. 1995; 41(1-3):241–248. https://doi.org/10.1016/0925-5273(94)00068-9

31. Brandon-Jones E, Squire B, Autry CW, Petersen KJ. A contingent resource-based perspective of supply chain resilience and robustness. Journal of Supply Chain Management. 2014; 50(3):55–73. https://doi.org/10.1111/jscm.12050

32. Tukamuhabwa BR, Stevenson M, Busby J, Zorzini M. Supply chain resilience: definition, review and theoretical foundations for further study. International Journal of Production Research. 2015; 53 (18):5592–5623. https://doi.org/10.1080/00207543.2015.1037934

33. Rahman S, Laosirihongthong T, Sohal AS. Impact of lean strategy on operational performance: a study of Thai manufacturing companies. Journal of manufacturing technology management. 2010; 21 (7):839–852. https://doi.org/10.1108/17410381011077946

34. Fretter C, Krumov L, Weihe K, Müller-Hannemann M, Hütt MT. Phase synchronization in railway timetables. European Physical Journal B. 2010; 77(2):281–289. https://doi.org/10.1140/epjb/e2010-00234-y

35. Huang Dw, Huang Wn. Traffic signal synchronization. Physical Review E. 2003; 67(5):056124. https://doi.org/10.1103/PhysRevE.67.056124 PMID: 12786237

36. Lämmer S, Kori H, Peters K, Helbing D. Decentralised control of material or traffic flows in networks using phase-synchronisation. Physica A: Statistical Mechanics and its Applications. 2006; 363(1):39–47. https://doi.org/10.1016/j.physa.2006.01.047

37. Treiber M, Helbing D. Macroscopic simulation of widely scattered synchronized traffic states. Journal of Physics A: Mathematical and General. 1999; 32(1):L17. https://doi.org/10.1088/0305-4470/32/1/003

38. Helbing D, Treiber M. Jams, waves, and clusters. Science. 1998; 282(5396):2001–2003. https://doi.org/10.1126/science.282.5396.2001

39. Helbing D. Traffic and related self-driven many-particle systems. Reviews of modern physics. 2001; 73 (4):1067. https://doi.org/10.1103/RevModPhys.73.1067

40. Becker T, Beber ME, Windt K, Hütt MT, Helbing D. Flow control by periodic devices: a unifying language for the description of traffic, production, and metabolic systems. Journal of Statistical Mechanics: Theory and Experiment. 2011; 2011(05):P05004. https://doi.org/10.1088/1742-5468/2011/05/P05004

41. Chankov S., Hütt M. & Bendul J. Understanding synchronizability of manufacturing networks: A multi-method study on structural network properties. Journal Of Manufacturing Systems. 2018; 46:127–136. https://api.semanticscholar.org/CorpusID:116823014 https://doi.org/10.1016/j.jmsy.2017.11.007

42. Arenas A, Díaz-Guilera A, Pérez-Vicente C. Synchronization Reveals Topological Scales in Complex Networks. Physical Review Letters. 2006; 96(11):114102. https://doi.org/10.1103/PhysRevLett.96.114102 PMID: 16605825

43. Buldyrev SV, Parshani R, Paul G, Stanley HE, Havlin S. Catastrophic cascade of failures in interdependent networks. Nature. 2010; 464(7291):1025–1028. https://doi.org/10.1038/nature08932 PMID: 20393559

44. De Domenico M, Granell C, Porter MA, Arenas A. The physics of spreading processes in multilayer networks. Nature Physics. 2016; (12):901–906. https://doi.org/10.1038/nphys3865

45. Yuan X, Hu Y, Stanley HE, Havlin S. Eradicating catastrophic collapse in interdependent networks via reinforced nodes. Proceedings of the National Academy of Sciences. 2017; 114:3311–3315. https://doi.org/10.1073/pnas.1621369114 PMID: 28289204

46. Klosik DF, Grimbs A, Bornholdt S, Hütt MT. The interdependent network of gene regulation and metabolism is robust where it needs to be. Nature Communications. 2017; 8(1):534. https://doi.org/10.1038/s41467-017-00587-4 PMID: 28912490

47. Chankov S, Hütt MT, Bendul J. Synchronization in manufacturing systems: quantification and relation to logistics performance. International Journal of Production Research. 2016; 54(20):6033–6051. https://doi.org/10.1080/00207543.2016.1165876

48. Chankov S, Hütt MT, Bendul J. Influencing factors of synchronization in manufacturing systems. International Journal of Production Research. 2017; p. 1–21. https://doi.org/10.1080/00207543.2017.1400707

49. Kauffman SA. Origins of Order: self-organization and selection in evolution; 1993. New York/Oxford: Oxford University Press.

50. Bak P, Tang C, Wiesenfeld K. Self-organized criticality: An explanation of the 1/f noise. Phys Rev Lett. 1987; 59:381–384. https://doi.org/10.1103/PhysRevLett.59.381 PMID: 10035754

51. Drossel B, Schwabl F. Self-organized criticality in a forest-fire model. Physica A-statistical Mechanics and Its Applications. 1992; 191:47–50. https://doi.org/10.1016/0378-4371(92)90504-J

52. Müller-Linow M, Marr C, Hütt MT. Topology regulates the distribution pattern of excitations in excitable dynamics on graphs. Phys Rev E. 2006; 74:016112. https://doi.org/10.1103/PhysRevE.74.016112

53. Pastor-Satorras R, Castellano C, Van Mieghem P, Vespignani A. Epidemic processes in complex networks. Reviews of Modern Physics, 2015; 87(3):925–979. https://doi.org/10.1103/RevModPhys.87.925

54. Messé A, Hütt MT, König P, and Hilgetag CC. A closer look at the apparent correlation of structural and functional connectivity in excitable neural networks. Scientific reports. 2015; 5(1):7870. https://doi.org/10.1038/srep07870 PMID: 25598302

55. Voutsa V, Battaglia D, Bracken LJ, Brovelli A, Costescu J, Diaz Munoz M, Fath BD, Funk A, Guirro M, Hein T et al. Two classes of functional connectivity in dynamical processes in networks. Journal of the Royal Society Interface. 2021; 18(183):20210486. https://doi.org/10.1098/rsif.2021.0486 PMID: 34665977

56. Hütt MT, Lesne A. In: Atay FM, Kurasov PB, Mugnolo D, editors. Unravelling Topological Determinants of Excitable Dynamics on Graphs Using Analytical Mean-field Approaches. Cham: Springer International Publishing 2020; 179–198. Available from: https://doi.org/10.1007/978-3-030-44097-8_9.

57. Barabási AL, Albert R. Emergence of scaling in random networks. Science. 1999; 286(5439):509–512. https://doi.org/10.1126/science.286.5439.509 PMID: 10521342

58. Müller-Linow M, Hilgetag CC, and Hütt MT. Organization of excitable dynamics in hierarchical biological networks. PLoS computational biology. 2008; 4(9):e1000190. https://doi.org/10.1371/journal.pcbi.1000190 PMID: 18818769

60. Hilgetag CC and Hütt MT. Hierarchical modular brain connectivity is a stretch for criticality. Trends in cognitive sciences, 2014; 18(3):114–115. https://doi.org/10.1016/j.tics.2013.10.016 PMID: 24268289

59. Garcia GC, Lesne A, Hütt MT, and Hilgetag CC. Building blocks of self-sustained activity in a simple deterministic model of excitable neural networks. Frontiers in computational neuroscience, 2012; 6:50. https://doi.org/10.3389/fncom.2012.00050 PMID: 22888317

61. Moretti P, Hütt MT. Link-usage asymmetry and collective patterns emerging from rich-club organization of complex networks. Proceedings of the National Academy of Sciences. 2020; 117(31):18332–18340. https://doi.org/10.1073/pnas.1919785117 PMID: 32690716

62. Erdős P, Rényi A. On random graphs. Publ Math (Debrecen). 1959; 6:290.

63. Brintrup A, Ledwoch A, Barros J. Topological robustness of the global automotive industry. Logistics Research. 2016 Dec; 9:1–7. https://doi.org/10.1007/s12159-015-0128-1

64. Becker T, Meyer M, Windt K. A manufacturing systems network model for the evaluation of complex manufacturing systems. International Journal of Productivity and Performance Management. 2014 Apr 8; 63(3):324–40. https://doi.org/10.1108/IJPPM-03-2013-0047

65. Funke T, Becker T. Complex networks of material flow in manufacturing and logistics: Modeling, analysis, and prediction using stochastic block models. Journal of Manufacturing Systems. 2020 Jul 1; 56:296–311. https://doi.org/10.1016/j.jmsy.2020.06.015

66. Messé A, Hütt MT, and Hilgetag CC. Toward a theory of coactivation patterns in excitable neural networks. PLoS computational biology. 2018; 14(4):e1006084. https://doi.org/10.1371/journal.pcbi.1006084 PMID: 29630592

67. Stricker N, Lanza G. The Concept of Robustness in Production Systems and its Correlation to Disturbances. Procedia CIRP. 2014; 19:87–92. https://doi.org/10.1016/j.procir.2014.04.078

68. He S, Li S, Ma H. Effect of edge removal on topological and functional robustness of complex networks. Physica A: Statistical Mechanics and its Applications. 2009; 388(11):2243–2253. https://doi.org/10.1016/j.physa.2009.02.007

69. Chan H, Akoglu L, Tong H. Make It or Break It: Manipulating Robustness in Large Networks. In: SDM; 2014. Available from: https://api.semanticscholar.org/CorpusID:15905240.

70. Beygelzimer A, Grinstein G, Linsker R, Rish I. Improving network robustness by edge modification. Physica A: Statistical Mechanics and its Applications. 2005; 357(3):593–612. https://doi.org/10.1016/j.physa.2005.03.040